



Study of the performance of Esparto grass fibers as adsorbent of dyes from aqueous solutions

Ridha Lafi^a, Nouredine Hamdi^b, Amor Hafiane^{a,*}

^aLaboratory of Wastewater Treatment, CERTE, BP 273, Soliman 8020, Tunisia, Tel. +216 79 325 750; Fax: +216 79 325 802; email: amor.hafiane@certe.rnrt.tn (A. Hafiane)

^bNational Centre of Research in Materials Sciences (CNRSM), BP95, 2050 Hammam-Lif, Tunisia

Received 5 February 2014; Accepted 21 June 2014

ABSTRACT

In this work, the sorption behavior of two basic dyes, Toluidine blue and Crystal violet (CV), on Esparto grass fibers *Stipa tenacissima* L., an abundant semi-arid region biomass was investigated. The surface properties of this new adsorbent were analyzed using various techniques such as FT-IR, BET, Differential scanning calorimetric, Boehm titration, and pH_{PZC} determination. Batch experiments were carried out to analyze the sorption kinetics and isotherms. The effect of operational parameters such as adsorbent dosage, dye concentration, ionic strength, pH, and temperature onto dye removal was studied. Under optimum conditions (25°C, pH 7.0, contact time of 150 min, and 2 g L⁻¹ adsorbent dose), the monolayer sorption capacities were about 40.00 mg g⁻¹ for TB and 43.47 mg g⁻¹ for CV. Equilibrium data were fitted to the Langmuir, Freundlich, and Temkin isotherm equations, and these data were found to be well represented by the Langmuir isotherm. The adsorption kinetics is represented by second-order kinetic model. Evaluated ΔG and ΔH specify the spontaneous and endothermic nature of the adsorption. The adsorption takes place with an increase in entropy (ΔS is positive). FT-IR spectrum was also taken to investigate the functional groups involved in the biosorption of cationic dyes. The obtained results indicated that *Stipa tenacissima* L. could be used to treat dye containing effluents.

Keywords: Adsorption; *Stipa tenacissima* L.; Basic dyes; Isotherm; Kinetics

1. Introduction

Wastewater generated by textile industries represents a major environmental concern. The discharge of the dye effluent in the environment is worrying for both toxicological and aesthetical reasons [1,2]. This dictates the necessity of the treatment of the dye containing water to undergo treatment before disposal to the environment. Various methods including coagulation–flocculation [3], oxidation [4,5], membrane

separation [6], and biological treatment [7] have been developed. Among these various water treatment technologies, adsorption has been found to be superior in term of initial cost, flexibility, and simplicity of design. Adsorption on activated carbon is widely used for the removal of dye and organic pollutants in general [8,9]. The high cost of activated carbon motivates the search for cheap materials from different biomass. Thus, several studies have shown that numerous low-cost materials have been successfully applied in the removal of dyes from aqueous solutions, some of

*Corresponding author.

which are *Posidonia oceanica* (L.) fibers [10], palm kernel fiber [11], orange waste [12], untreated coffee residues [13], date pits solid adsorbent [14], peanut husk [15], bagasse [16], hen feathers [17], bottom ash [18], and de-oiled soya [19].

Esparto grass fibers (EGF, *Stipa tenacissima* L: Alfa) is a tussock grass widely distributed in semi-arid and arid regions, in North Africa and southern Spain [20]. In Tunisia, it covers area of 475,829 ha [21], mainly located in Kasserine, Sidi Bouzid, Gafsa, and Kairouan region. Alfa is considered as one of the most interesting annual plants for the production of fibers for papermaking and the production of Alfa pulp exceeds 30,000 tons per year [22].

EGF was used as precursor for the production of activated carbon by chemical activation using KOH solutions [23] and by physical activation with carbon dioxide [24]. Alfa plant is a complex material composed of 45% cellulose, 25% hemicellulose, 23% lignin, 5% wax, and 2% ash [25]. Cellulose is a linear polymer insoluble in water with β -D-glucopyranose units; hemicellulose is a chemically ill-defined polysaccharide with low molecular weight, so it can be dissolved in water [26]. Both cellulose and hemicellulose contain majority of oxygen functional groups which are present in the lignocellulosic material such as hydroxyl, ether, and carbonyl groups, while lignin is a complex, systematically polymerized, highly aromatic substance, and acts as a cementing matrix that holds between and within both cellulose and hemicellulose units [26]. These polymers are rich in carboxyl and hydroxyl functional groups, which possibly may bind cationic dye molecules in aqueous [22].

Therefore, the objective of this study was to evaluate the adsorption potential of EGF for two cationic dyes, crystal violet (CV) and toluidine blue (TB), which were chosen as cationic dyes models. CV belonging to triphenylmethane group and has been widely applied in coloring paper, temporary hair colorant, dyeing cottons, and wools. It can cause some harmful effects, such as heartbeat increase, vomiting, shock cyanosis, jaundice, quadriplegia, and tissue necrosis in humans [27]. TB, a phenothiazine type dye, has been widely used for different purposes in several fields such as medicine, textiles, and biotechnology [28]. TB has a mutagenic effect, has toxic in the level of organism, cell, and has toxic interaction with RNA. TB can significantly decrease the mean half-life of motile bull spermatozoa and can induce structural changes of rat mast cells [29]. In this study, the effect of key operating parameters such as initial pH, ionic strength, dye concentration, and temperature were investigated. The kinetic data were fitted with pseudo-first-order and pseudo-second-order kinetic models.

The Langmuir, Freundlich, and Temkin models were used to describe the equilibrium isotherms. Finally, an attempt was made to describe the mechanism of adsorption.

2. Experimental

2.1. Adsorbent

The EGF (*Stipa tenacissima*, L) used as an adsorbent in this study was collected from Sidi Bouzid, south west of Tunisia. The EGF was allowed to dry for three months in free air. The raw fiber are cut into small chips, washed several times with distilled water, and then dried in an oven at 80°C. The dried materials were then crushed and sieved to obtain the particle size inferior to 250 μm ; the resulting product was stored in air-tight container for further use.

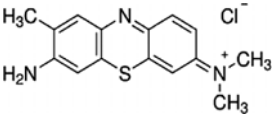
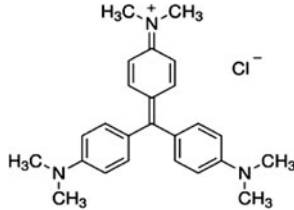
2.2. Chemicals

Chemicals including NaOH, HCl, Na_2CO_3 , NaHCO_3 , NaCl, TB, and CV with analytical grade are purchased from Merck. The characteristics and chemical structures of TB and CV are listed in Table 1. The stock solutions of 1,000 mg L^{-1} dyes solutions were prepared and the solutions of desired dye concentration were prepared by successive dilution of the stock solution with distilled water.

2.3. Characterization of Esparto grass fiber

Analytical methods, used to characterize the EGF, include S_{BET} , Differential scanning calorimetric (DSC), Fourier Transform infrared spectroscopy (FTIR), Boehm titration, and point of zero charge (PZC). The surface area, total pore volume, and average pore diameter of the EGF were determined from the adsorption isotherms of nitrogen at 77 K using a surface analyzer Autosorb1 (Quantachrome instruments). DSC analyses were performed using a DSC 4000 analyzer from Perkin-Elmer. The sample of 5.6 mg was heated from 0 to 450°C at a heating rate of 20°C min^{-1} . The FTIR analysis was done using a Fourier transform spectrophotometer model IRAffinity-1S from SHIMADZU. The spectra of the EGF before and after adsorption were in a range of 4,000–400 cm^{-1} . The determination of surface functional groups was based on the Boehm titration method. Aqueous solutions of NaHCO_3 (0.10 mol L^{-1}), Na_2CO_3 (0.05 mol L^{-1}), NaOH (0.10 mol L^{-1}), and HCl (0.10 mol L^{-1}) were prepared. A volume of 25 mL of these solutions was added to 0.5 g of EGF, shaking for 48 h at room temperature, and then filtered. The

Table 1
The characteristics and chemicals structure of dyes

Dye name	Toluidine blue	Crystal violet
Abbreviation	TB	CV
Color index number	52040	42555
Molecular formula	$C_{15}H_{16}ClN_3S$	$C_{25}H_{30}ClN_3$
Molecular weight	305.8 g mol ⁻¹	408 g mol ⁻¹
λ_{max} (nm)	623	590
Chemical name	3-Amino-7-(dimethylamino)-2-Methylphenothiazin-5-ium chloride	Hexamethylpararosanine chloride
Molecular structure		

excess of base or acid was then determined by back titration using NaOH (0.10 mol L⁻¹) and HCl (0.10 mol L⁻¹) solutions. The number of acidic sites was determined under the assumptions that NaOH neutralizes carboxylic, lactonic, and phenolic groups, that Na₂CO₃ neutralizes carboxylic and lactonic groups, and that NaHCO₃ neutralizes only carboxylic groups. The test was repeated at least three times. The PZC of EGF was determined by known mass titrations method [30].

2.4. Batch adsorption studies

Adsorption studies were performed in batch to obtain the rate and the equilibrium data. Experiments were carried out by contacting fixed amount of EGF (0.2 g) with 100 mL of dye solution of different initial concentrations (20–100 mg L⁻¹) in 250 mL Erlenmeyer flasks without changing pH (pH 7) and temperature (25 ± 1°C). These flasks were agitated at 220 rpm.

The amount of adsorption at equilibrium, q_e (mg g⁻¹), and the dye removal percentage (%) for two dyes, CV and TB, were determined using thermo spectronic UV 1 Spectrophotometer at 590 and 623 nm wavelengths, respectively.

The effect of EGF dose on the adsorption process was investigated by contacting 100 mL of dye solution of initial concentration of 20 mg L⁻¹ with different amount of EGF into a number of 250 mL Erlenmeyer flasks at temperature of 25 ± 1°C and at pH 7. The flasks were agitated at 220 rpm for 150 min.

To investigate the effect of pH on biosorption, a series of dye solutions were prepared by adjusting the pH over a range of 2.5–10 using HCl or NaOH

solutions. In this study, 100 mL of initial dye concentration of 20 mg L⁻¹ was added to 0.2 g of adsorbent and then the mixture is agitated during 150 min at 25 ± 1°C.

3. Results and discussion

3.1. Adsorbent characterization

PZC and concentration sites of EGF are presented in Table 2. The PZC of an adsorbent is an important characteristic that determines the pH at which the adsorbent surface has net electrical neutrality. The PZC value is around 6.3 and therefore, pH values should be maintained above 7 to ensure a predominant negatively charged surface. At lower pH values, the surface charge may get positively charged, making H⁺ ions compete effectively with the cationic CV and TB dyes. The BET surface area, total pore volume, and average pore diameter of the EGF were found to be 20.7 m² g⁻¹, 0.11 cm³ g⁻¹, and 20.57 nm, respectively. These results indicated that this material has very low surface area and small pore volume.

The nitrogen adsorption isotherms at 77 K, shown in Fig. 1, are of type II, according to the IUPAC classification system and typical of macroporous or

Table 2
PZC and concentration sites of EGF

PZC	Acidic groups (m mol g ⁻¹)					
	Carboxylic	Lactonic	Phenolic	Acid	Basic	Total
6.3	0.58	0.03	0.96	1.57	0.4	1.97

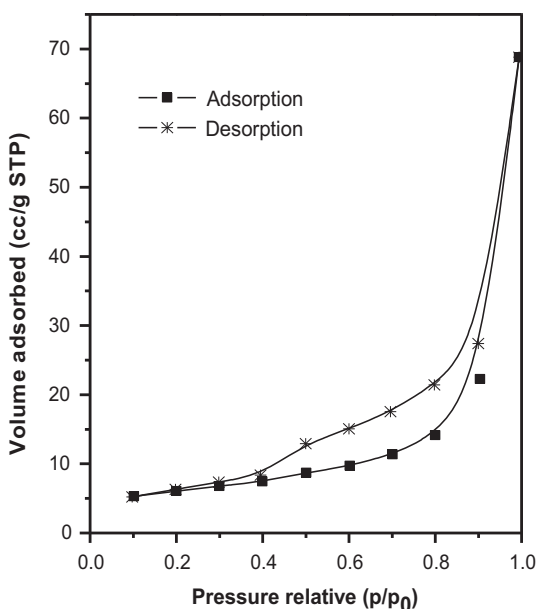


Fig. 1. Nitrogen adsorption–desorption isotherm of EGF.

non-porous adsorbents. The hysteresis was of H3 type, characteristic of fibers materials with slit-shaped pores [31].

The thermal degradation of the precursor was studied by DSC under nitrogen flow. Fig. 2 indicates the presence of cellulose by one big endothermic curve at 81.4°C; caused by evolution of water entrapped by OH-groups present in cellulosic chains. The

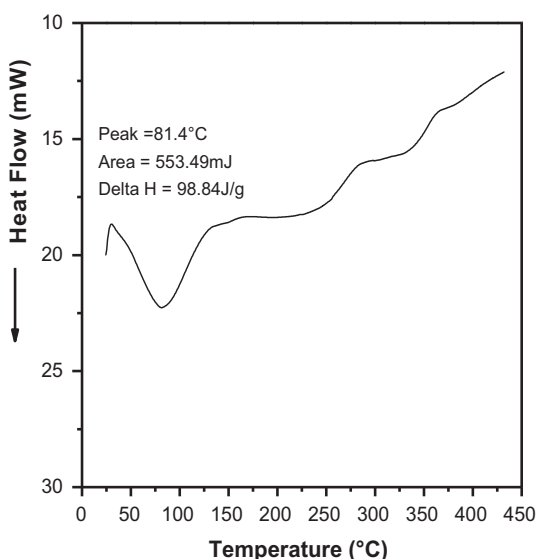


Fig. 2. Thermal degradation by differential scanning calorimetry.

Table 3

Characterization of Esparto grass

Elemental analysis (wt%)	C	44.3
	H	6.5
	N	0.6
	O	46.5
	S	<1d
Cellulose (wt%)		45.3
Hemicellulose (wt%)		23.7
Lignin (wt%)		23.9
Ash (wt%)		2.1
Waxes (wt%)		5.0

Note: <1d, below detection limit.

cellulose decomposition takes place at temperatures higher than 200°C. The results of the elemental composition of EGF presented in Table 3 showed that cellulose is the major component, followed by hemicelluloses and lignin. The smallest components are waxes and ashes.

The contents of carbon, hydrogen, and oxygen were similar to those previously reported in the case of other lignocellulosic materials such as *Posidonia oceanica* (L.) [32], *piassava fibers* [33], and *Euphorbia rigida* [34], which have a content of C = 42–49%, H = 5.1–6.4%, and O = 34–46%.

The FT-IR spectra of E. grass fiber were recorded before and after dyes biosorption (Fig. 3 and Table 4). The first part of the spectra (in the range 4,000–2,800 cm^{-1} , Fig. 3(a)) indicated: (i) a broad band in the range of 3,700–3,000 cm^{-1} which represents different modes of vibration such as the free OH, OH stretch, and interchain H-bonds, (ii) two small peaks at 2,918 and 2,844 cm^{-1} that correspond to symmetric $-\text{CH}_2$ valence vibration and $-\text{CH}$ stretching vibration, respectively [35]. As it is generally difficult to find useful information from this range of wavenumber, spectrum analysis will be focused on the second range of spectra (1,800–600 cm^{-1} , Fig. 3(b)). A band observed at 1,653 cm^{-1} is attributed to C=O stretch in conjugated p-substituted aryl ketones [35]. On this broad band, a shoulder can be observed at 1,721 cm^{-1} : this is representative of either C=O stretch in unconjugated ketones, carbonyls, and in ester groups (especially in carbohydrates) conjugated aldehydes and carboxylic acids, or C=O valence vibration of acetyl or COOH groups.

The band at 1,514 cm^{-1} can be identified in amine/ amide groups and in carboxyl groups. A series of bands are identified in the range of 1,430–1,300 cm^{-1} ; they are non-specific bands that can be readily identified in cellulose material (1,427, 1,381, and 1,321 cm^{-1}) because the biopolymer is more crystalline than other constituents of hemicelluloses and lignin [36]. Another

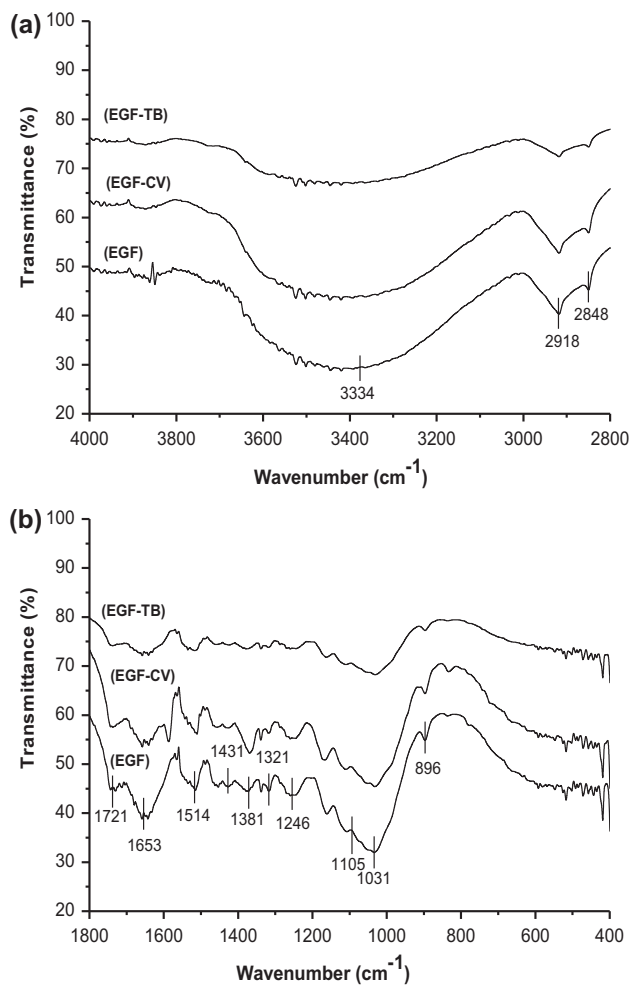


Fig. 3. FTIR spectra of EGF, EGF-CV, and EGF-TB.

Table 4
FTIR spectral characteristics of EGF

Frequency (cm^{-1})			Assignment
Before adsorption	After adsorption TB	After adsorption CV	
3,334	3,344	3,344	Bonded O–H groups
2,918	2,918	2,918	Aliphatic C–H groups
2,848	2,848	2,850	CH_2 groups
1,726	1,731	1,737	C=O stretching
1,653	1,658	1,666	COOH bending
		1,587	C–N
1,514	1,512	1,514	C–C=C groups
1,431	1,427	1,437	CH_2
1,381	1,377	1,369	C–O–H bending
1,246	1,244	1,244	C–O stretching
1,161	1,163	1,166	C–O–C stretching
1,033	1,031	1,031	C–O stretching
896	896	896	C–C groups

broad band appears at $1,246 \text{ cm}^{-1}$ that was attributed to symmetric stretching in carboxyl groups. The band around $1,105 \text{ cm}^{-1}$ represented of carbohydrate ring bonds. The band at $1,033 \text{ cm}^{-1}$ can be due to C–O–C stretching of phenolic groups of cellulose. The band at 896 cm^{-1} can be probably attributed to anomer C-groups and ring valence vibration [35]. The FTIR spectra of CV-sorbed EGF showed that the bands at $3,334, 1,721, 1,653, 1,431, 1,381,$ and $1,161 \text{ cm}^{-1}$ had shifted to $3,344, 1,737, 1,666, 1,437, 1,369,$ and $1,166 \text{ cm}^{-1}$ after CV biosorption. These observed shifts indicate that an interaction was occurred between CV molecules and the carboxylate and the hydroxylate anions. Thus, the contribution of the carboxyl and hydroxyl groups seems to be predominant in the absorption of the dye. Finally, the appearance of new peak at $1,587 \text{ cm}^{-1}$ may be attributed to the C–N group of dye after biosorption [37].

In the case of TB also, the peaks at the bands at $3,334, 1,721, 1,653, 1,431, 1,381,$ and $1,161 \text{ cm}^{-1}$ shifted to $3,344, 1,731, 1,658, 1,427, 1,377,$ and $1,163 \text{ cm}^{-1}$ after TB biosorption. These shifts in the peaks indicate that an interaction occurred between TB molecules and carboxylate and the hydroxylate anions.

3.2. Effect of adsorbent dose

The effect of biosorbent mass quantity was studied by varying the quantity of EGF in the range of $0.1\text{--}10 \text{ g L}^{-1}$, whereas the parameters such as initial dye concentration, contact time, pH of the solution, stirring rate, and temperature were all kept constant during the adsorption process. It is apparent from Fig. 4 that by

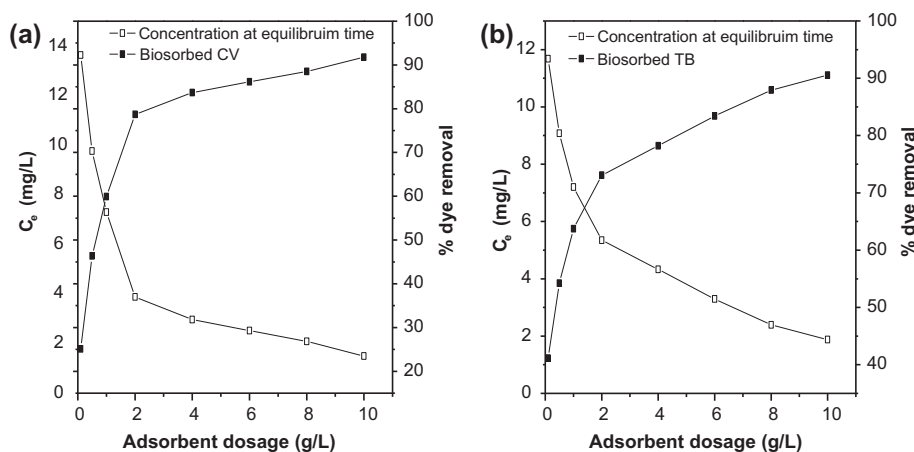


Fig. 4. Effect of adsorbent dosage on CV and TB adsorption onto EGF (initial dye concentration: 20 mg L^{-1} , temperature 25°C , and pH 7).

increasing the adsorbent dose from 0.1 to 10 g L^{-1} , the percentage of dye removal increased from 25 to 91% for CV and from 41 to 90% for TB. This could be attributed to an increase in the adsorbent surface area and thereby the number of adsorption sites available for adsorption. The slower rise in dye removal efficiency observed after the initial increase is probably due to the aggregation of biosorbent particles by increasing biosorbent dose. Such aggregation decreased the effective surface area of biosorbent [38].

3.3. Effect of pH

One of the most important factors influencing the biosorption of dye on a biosorbent is the pH of the adsorbate solution; pH affects the availability of dye molecules for a possible adsorption on EGF and also influences the activities of functional groups on the biosorbent surface [15]. The removal percentage of TB and CV as function of pH is shown in Fig. 5(a). In the case of TB, the percentage removal increased from 35.1% (at pH 2.8) to 91.2% (at pH 7.0), whereas in the case of CV, the adsorption percentage increase from 41.8% (at pH 2.6) to 85.2% (at pH 7.0). Lower dye removal percentage at acidic pH may be due to the presence of an excess of H^+ ions competing with cationic dyes for adsorption sites. At a higher pH solution, the biopolymer fibers, mainly lignin, and cellulose chains, may get negatively charged, which enhances the adsorption of the positively charged dyes through electrostatic forces of attraction.

3.4. Effect of contact time

The effect of contact time was monitored for different initial dye concentration (20, 40, 60, 80, and

100 mg L^{-1}) and pH 7. Both dyes show a fast rate of adsorption during the first 60 min of the dye-adsorbent contact (Fig. 6). At higher contact time, the rate of adsorption decreases gradually leading to equilibrium at about 150 min. At the beginning, the dye ions were adsorbed by the exterior surface of EGF, the biosorption rate was very fast. When the adsorption of the exterior surface of EGF reached saturation, the dye ions entered into the pores of EGF and were adsorbed by the interior surface of the particles [39]. Fig. 6 shows also that increase in the initial dye concentration leads to an increase in the adsorption capacity of the dye on EGF. The adsorption capacity at equilibrium increases from 8.8 to 29.5 mg g^{-1} for CV and from 8.3 to 27 mg g^{-1} for TB with an increase in the initial dye concentration from 20 to 100 mg L^{-1} . The adsorption of MB and CV onto other lignocellulose adsorbent follows the same trend [10,11].

3.5. Effect of ionic strength

Since large amounts of salts are generally utilized in the dyeing process, the effects of ionic strength on adsorption must be evaluated. Generally, an increase in ionic strength decreases the adsorption capacity when electrostatic interactions between adsorbent and adsorbate are attractive, as in our study, but increases the adsorption capacity when they are repulsive [40].

The effect of ionic strength on the adsorption of dyes onto EGF was investigated by the addition of different amounts of sodium chloride ranging from 0 to 40 g L^{-1} . As seen in Fig. 5(b), increasing the ionic strength of solution decreases the adsorption of dyes. This could be attributed to the competition of dye cations and Na^+ ion for sorption sites. The effect of ionic

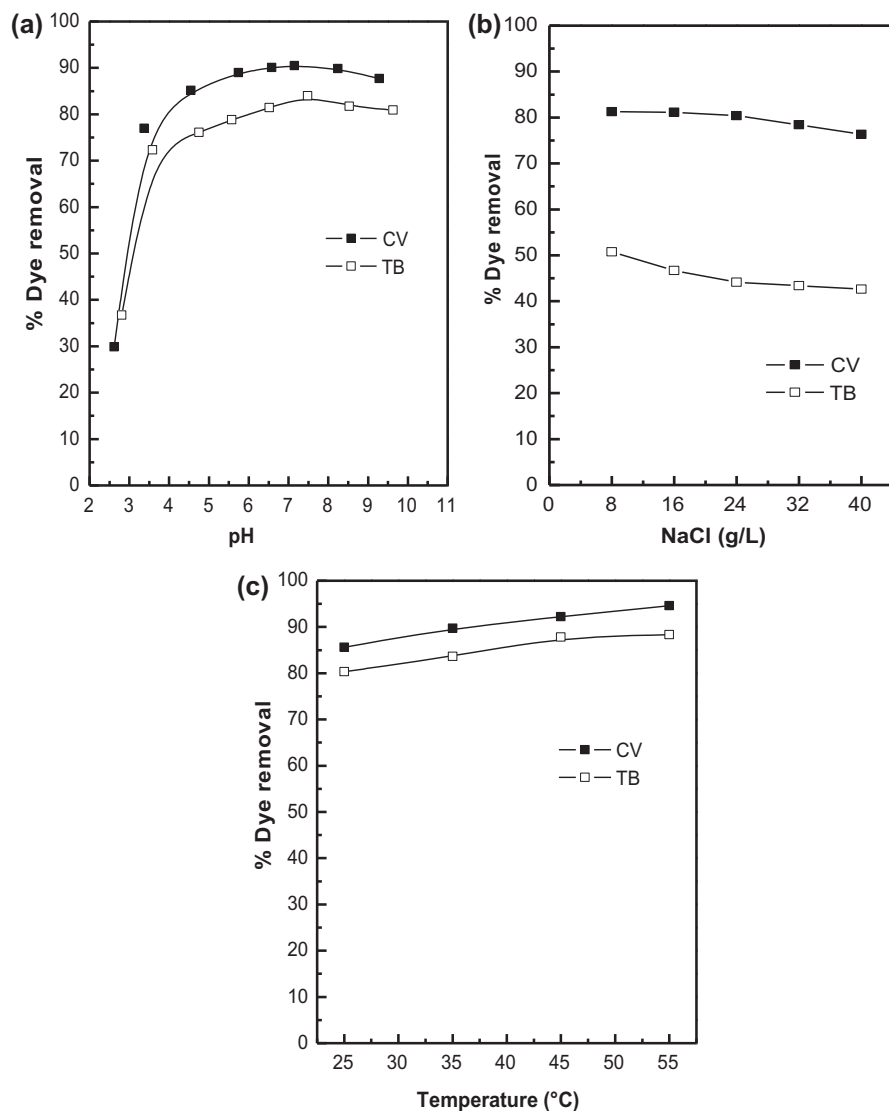


Fig. 5. Effect of (a) solution pH, (b) NaCl, and (c) temperature adsorption of TB and CV on EGF.

strength on adsorption of CV was more remarkable. In this case, the contribution of electrostatic attraction on dye-adsorbent is more important [41].

3.6. Effect of temperature

The effect of temperature on the adsorption of CV and TB on EGF was carried out at different temperatures 25, 35, 45, and 55 °C. As seen in Fig. 5(c), the increase of temperature from 25 to 55 °C induces the increase dye removal percentage from 85.6 to 94.6% for CV and from 80.3 to 88.3% for TB. This may be due to the increase of the mobility of the dye molecules by increasing the temperature [11]. This phenomenon indicates that the adsorption process is endothermic.

3.7. Adsorption isotherms modeling

The equilibrium sorption isotherm is fundamental in describing the interactive behavior between adsorbent and adsorbate and is important in the design and analysis of sorption systems. The most common models used to represent the data of adsorption from solution are Langmuir [42], Freundlich [43], and Temkin [44] isotherms.

In this work, these models (Fig. 7) were used to discuss the equilibrium characteristics of the adsorption process. The applicability of the isotherm models to the adsorption study within the experimental conditions (concentration range 20–180 mg L⁻¹, adsorbent dose 2 g L⁻¹, temperature 25 ± 1 °C, contact time 150 min, and stirring speed 220 rpm) was judged by

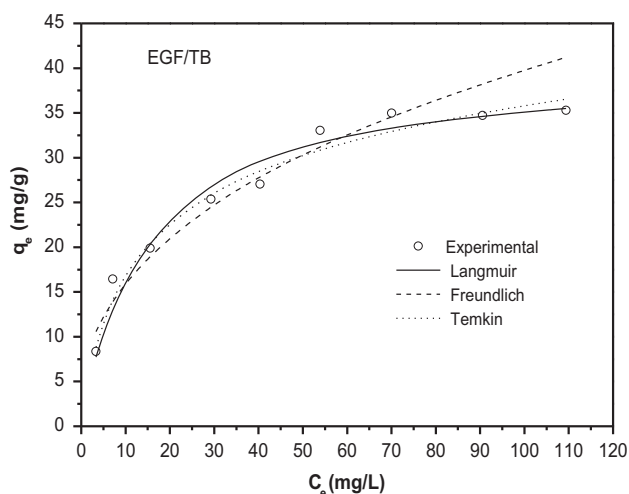
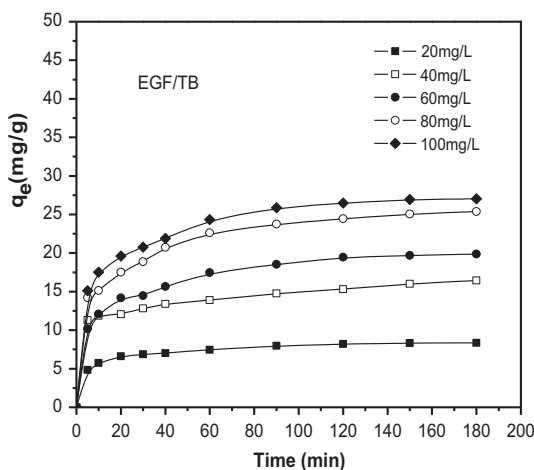
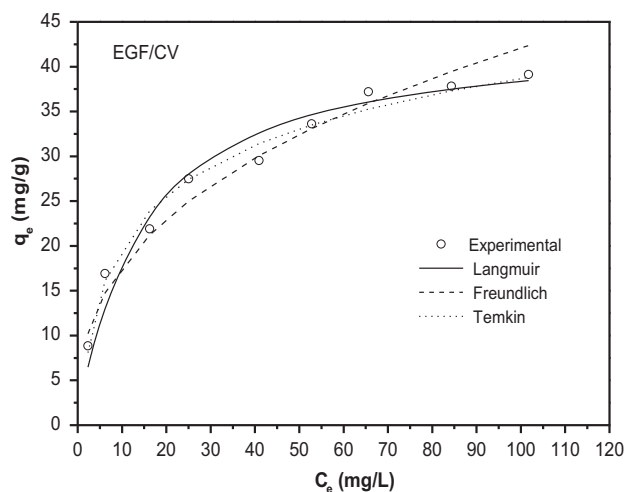
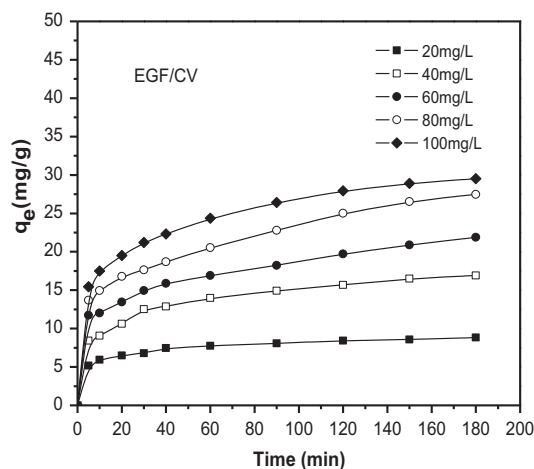


Fig. 6. Effect of initial concentration and contact time on the adsorption of TB and CV ($C_0 = 20\text{--}100\text{ mg L}^{-1}$, EGF dosage = 0.2 g, temperature = 25°C, $t = 180\text{ min}$, rpm = 220, and pH 7).

Fig. 7. Isotherm modeling of CV and TB adsorption onto EGF at 25°C.

the value of R^2 correlation coefficient of each plot. Langmuir isotherm assumes monolayer adsorption onto a homogeneous surface containing a finite number of adsorption sites of adsorption with no transmigration of adsorbate in the plane of surface. In order to establish the maximum sorption capacity, the Langmuir equation was applied. In this model, q_e is the amount adsorbed at equilibrium (mg g^{-1}), C_e is the equilibrium concentration of the adsorbate (mg L^{-1}), and q_{max} (mg g^{-1}) and K_L are the Langmuir constants related to the maximum adsorption capacity and the energy of adsorption, respectively. These constants can be evaluated from the intercept and the slope of the linear plot of experimental data of C_e/q_e vs. C_e . The essential characteristics of the Langmuir isotherm can be expressed by dimensionless equilibrium parameter (R_L) [45]. The R_L parameter indicates the type of the isotherm as follows: $R_L > 1$,

unfavorable; $R_L = 1$, linear; $0 < R_L < 1$, favorable; $R_L = 0$, irreversible. Values of R_L were found to be 0.396–0.116 for CV and 0.408–0.121 for TB in the concentration range studied. These results confirmed that the EGF is favorable for the adsorption of dye under the used experimental conditions.

The Freundlich isotherm model is derived by assuming a heterogeneous surface with a non-uniform distribution of heat of adsorption over the surface. In this model, K_F (mg g^{-1}) and n are Freundlich model constants related to the capacity and intensity of the adsorption, respectively. The values of K_F and $1/n$ can be obtained from the intercept and slope, respectively, from the linear plot of experimental data of $\ln q_e$ vs. $\ln C_e$.

The Temkin isotherm assumes that the heat adsorption of all molecules in the layer decreases linearly with coverage due to the adsorbent–adsorbate interaction. It also assumes that adsorption characterized by a

uniform distribution of bending energies up to some maximum value. B is the constant related to the energy of adsorption (J/mol) and A is the Temkin isotherm constant (L/g). B and A could be calculated from the linear plot of $\ln C_e$ against q_e .

Table 5 summarizes the results of the isotherm constants for the three equilibrium isotherms tested. On the basis of the correlation coefficients R^2 , Langmuir isotherm represents the equilibrium adsorption data with better fit ($R^2 = 0.99$) as compared to the other isotherms.

3.8. Adsorption kinetics studies

The kinetics of TB and CV adsorption on the EGF was analyzed using pseudo-first [46], pseudo-second-order [47]. The equations of each model in addition to their obtained constants are reported in Table 6. For the pseudo-first-order model, k_1 represents the rate constant and q_e denotes the amount of adsorption at equilibrium. Plotting $\log(q_e - q_t)$ against t permits

calculation of k_1 (Fig. 8). For the pseudo-second-order kinetic, k_2 is the rate constant of pseudo-second-order equation. Plotting t/q_t against t gives a straight line (Fig. 9) where k_2 can be calculated.

The results of fitting experimental data with the pseudo-first-order and pseudo-second-order models for adsorption of TB and CV on EGF are presented in Table 6. As seen in this table, the correlation coefficients R^2 for the linear plots of the pseudo-second-order is 0.99 which is higher than that obtained in pseudo-first-order model. In addition, the calculated values of q_e are in agreement with experimental q_e values. This indicates that the adsorption kinetics is better represented by the pseudo-second-order model.

Intraparticle diffusion model introduced by Weber and Morris was studied to investigate the diffusion mechanism of adsorption process [48]. In this model, k_{id} is the intraparticle diffusion rate constant ($\text{mg g}^{-1} \text{min}^{1/2}$) determined from the slope of the plot q vs. $t^{0.5}$. Fig. 10 shows that the linear plot did not pass through the origin which indicated that the

Table 5
Isotherm parameters for adsorption of CV and TB onto EGF

Adsorption isotherm	Adsorption constant	Type of dyes	
		TB	CV
Langmuir $\frac{C_e}{q_e} = \frac{1}{q_{\max} b} + \frac{C_e}{q_{\max} b}$	q_{\max} (mg g^{-1})	40.00	43.47
	b (mg L^{-1})	0.072	0.076
	R_L	0.408–0.121	0.396–0.116
	R^2	0.99	0.99
Freundlich $\ln q_e = \ln K_F + \frac{1}{n} \ln C_e$	n	2.57	2.65
	K_F (mg g^{-1})	6.43	7.44
	R^2	0.94	0.98
Temkin $q_e = B \ln A + B \ln C_e$	A	0.91	1.17
	B	7.92	8.11
	R^2	0.97	0.98

Table 6
Kinetic parameters for adsorption of CV and TB onto EGF

Dye	C_0 (mg L^{-1})	Pseudo-first-order kinetics			Pseudo-second-order kinetics			Intraparticle diffusion		
		$\log(q_e - q_t) = \log(q_e) - \left(\frac{k_1}{2.303}\right)t$	$\frac{t}{q_t} = \frac{1}{k_2 q_e^2} + \frac{t}{q_e}$	q_e (mg g^{-1})	k_1 (min^{-1})	R^2	q_e (mg g^{-1})	k_2 (g mg min^{-1})	R^2	C
CV	20	4.16	0.019	0.95	9.04	0.014	0.99	5.05	0.305	0.96
	40	9.58	0.016	0.95	17.32	0.004	0.99	7.51	0.372	0.97
	60	13.07	0.015	0.95	22.47	0.003	0.99	9.55	0.928	0.99
	80	18.31	0.017	0.97	28.80	0.002	0.99	10.91	1.257	0.99
	100	18.03	0.021	0.98	30.81	0.002	0.99	13.81	1.257	0.98
TB	20	4.37	0.029	0.97	8.63	0.017	0.99	4.41	0.401	0.96
	40	7.05	0.016	0.89	16.69	0.007	0.99	8.38	0.479	0.99
	60	10.46	0.027	0.98	20.85	0.004	0.99	10.20	1.127	0.98
	80	14.45	0.024	0.97	26.44	0.004	0.99	11.14	1.409	0.98
	100	15.75	0.028	0.98	28.19	0.004	0.99	12.62	1.458	0.96

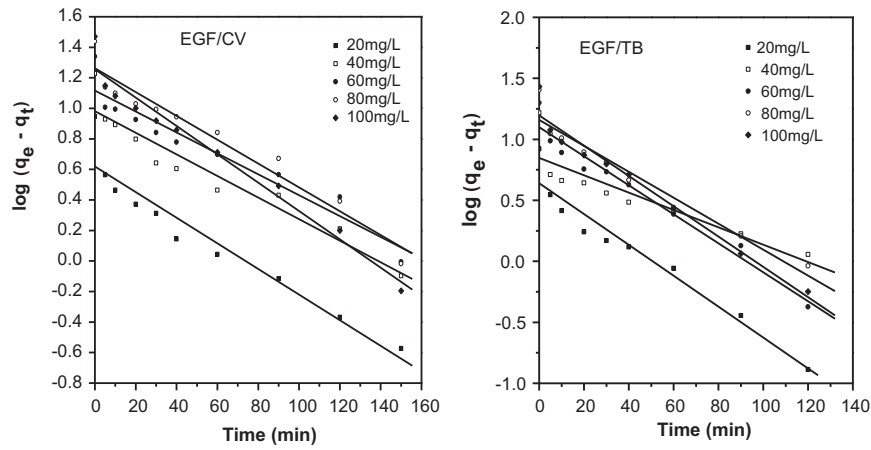


Fig. 8. Plots of pseudo-first-order of CV and TB adsorption onto EGF at 25°C.

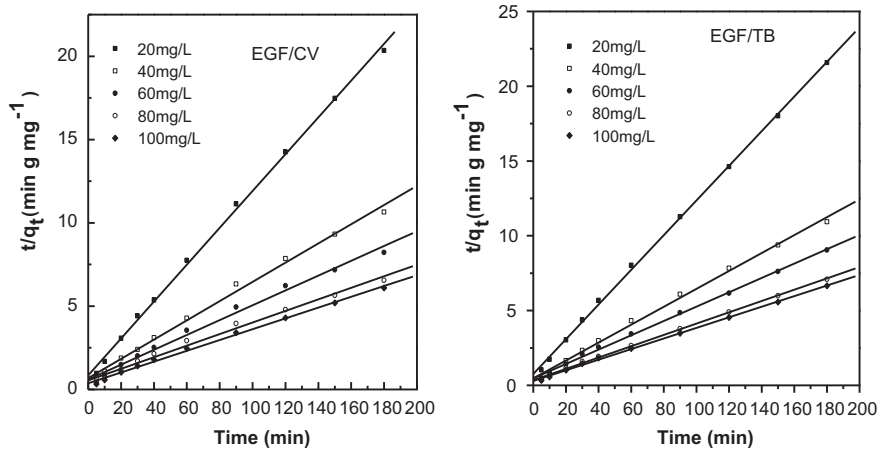


Fig. 9. Plots of pseudo-second-order of CV and TB adsorption onto EGF at 25°C.

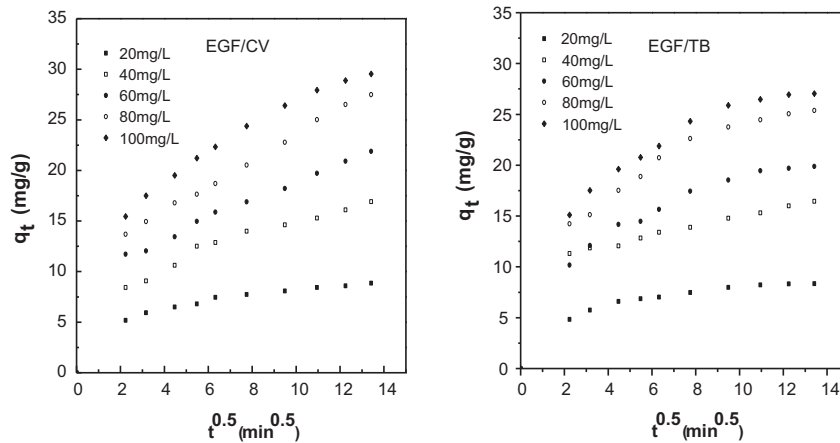


Fig. 10. Intraparticle diffusion of CV and TB adsorption onto EGF at 25°C.

intraparticle diffusion was not the only rate-controlling step for the adsorption of TB and CV. Thus, two stages for dyes adsorption can be distinguished. The first stage is an instantaneous adsorption and is probably due to a strong electrostatic attraction between dye and external surface of adsorbent. The second stage is a gradual adsorption stage, which can be attributed to intraparticle diffusion of dye molecule through the pores of adsorbent. The k_{id} values (Table 6) should be calculated based on the data corresponding to this stage [49].

3.9. Thermodynamics parameters

To further understand the adsorption process taking place between dyes and EGF adsorbent, thermodynamic parameters were evaluated (Table 7). The following Van't Hoff equation was used to calculate the values of enthalpy (ΔH) and entropy (ΔS).

$$\ln k_0 = \frac{-\Delta G}{RT} = \frac{-\Delta H}{RT} + \frac{\Delta S}{R} \quad (1)$$

where $K_0 = q_e/C_e$ is the equilibrium constant (L/mg) of adsorption process at temperature T , R is the gas constant ($8.314 \text{ J mol}^{-1} \text{ K}$), and T is temperature (K). The plot of $\ln K_0$ as a function of $1/T$ (Fig. 11) yields a straight line ($R^2 \geq 0.99$ for CV and TB) from which ΔH and ΔS were calculated from the slope and intercept, respectively.

The Gibbs free energy (ΔG) was calculated to determine the feasibility of adsorption using the equation:

$$\Delta G = -RT \ln(K_0) \quad (2)$$

For both dyes, the ΔG values were negative across all temperatures (Table 7) inferring the spontaneous in nature of adsorption of dyes onto EGF. The positive value of ΔH for CV and TB confirmed the endothermic nature of the adsorption process, while the positive value of ΔS suggested an increase in the

Table 7
Thermodynamic parameters for the adsorption of CV and TB onto EGF

Dye	ΔH° (kJ mol ⁻¹)	ΔS° (kJ mol ⁻¹)	$-\Delta G^\circ$ (kJ mol ⁻¹)			
			298 K	308 K	318 K	328 K
CV	28.90	0.10	2.68	3.74	4.79	5.85
TB	17.85	0.06	2.31	2.99	3.66	4.34

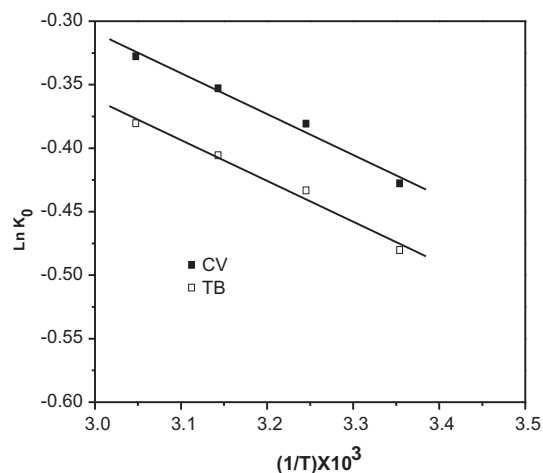


Fig. 11. Thermodynamic parameters for adsorption of CV and TB on EGF.

randomness at the solid–solution interface during the adsorption of dyes onto EGF.

3.10. Biosorption mechanism

The major components of EGF biomass are cellulose (45.3%), lignin (23.9%), and hemicellulose (23.7%). Cellulose is characterized by a linear structure made of β (1→4) linked D-glucose units associated to other chains through hydrogen bonds; it is also rich in hydroxyl groups, the polymer contains three hydroxyl groups at C-2, C-3, and C-6 atoms representing a favorable characteristic of EGF to be a potential adsorbent material. Lignin is characterized by the presence of phenolic hydroxyl, aliphatic hydroxyl, methoxyl, and carbonyl functional groups. Hemicellulose is constituted of different heteropolysaccharides (xylose, mannose, galactose) associated on a disorganized (non-linear, ramified) mode with other polysaccharides and with lignin.

The functional groups of EGF which may play a role in the adsorption process were determined by FTIR spectroscopy. The spectra of EGF and dye-adsorbed EGF were shown in Fig. 3 representing the complex nature of the adsorbent.

Most changes occurring on the biosorbent after biosorption of dyes are reflected in the broad band present between $3,200$ and $3,700 \text{ cm}^{-1}$. This may be attributed to the interaction of dyes with the ionized O–H group of “free” hydroxyl groups and bonded O–H bands of carboxylic acids in the intra- and intermolecular hydrogen bonding of polymeric compounds (macromolecular associations), such as alcohols, phenols, and carboxylic acids, as in pectin, cellulose, and lignin [50].

The changes in peaks observed between 1,740 and 1,720 cm^{-1} are indicative of stretching vibration of C=O bonds due to non-ionic carboxyl groups of pectin and may be probably assigned to hydrogen bonding between carboxylic acids or their esters and dyes molecules [50].

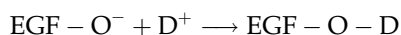
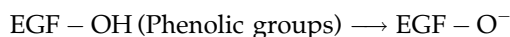
The peaks observed between 1,670 and 1,650 cm^{-1} are attributed to the stretching vibration of the asymmetric and symmetric COO^- of deprotonated

carboxylate functional groups of lignin [50]. These changes can be due to electrostatic interaction between carboxylate anions and cationic dye.

The change in peaks observed between 1,385 and 1,370 cm^{-1} may be assigned to binding hydroxyl groups ($-\text{C}-\text{O}-\text{H}$) of cellulose to dyes molecules [50].

The adsorption was strongly pH dependent. CV and TB were adequately adsorbed for pH between 7.0 and 9.5. It was also observed that the modeling of intraparticle diffusion showed a contribution of film diffusion on the control of sorption kinetics; however, intraparticle diffusion was not the dominating mechanism.

On the basis of the FTIR spectrum and active site analysis, the adsorption mechanism of dyes onto EGF may be assumed to involve three steps: (i) migration of dyes from the solution to EGF surface and diffusion of dyes to the surface, (ii) adsorption of dyes on the surface, which may be due to the formation of surface hydrogen bonds between the hydroxyl groups on the surface of the adsorbent and the nitrogen atoms of dyes as suggested in Fig. 12 or through a possible mechanism of dye–hydrogen process as shown below:



(iii) Intraparticle diffusion of dyes into the interior pores of the adsorbent.

3.11. Comparison of EGF with other sorbents

Table 8 summarizes the comparison of the maximum CV and TB adsorption capacities of various sorbents including EGF. The comparison shows that EGF has higher adsorption capacity of CV and TB than many of the other reported adsorbents. The

Table 8

Comparison of the adsorption capacity of basic dyes with different various adsorbent

Dye	Adsorbent	q_{max} (mg g^{-1})	References
CV	Palm kernel fiber	78.9	[11]
	Tomato plant root	94.3	[51]
	Grapefruit peel	249.6	[52]
	Neem sawdust	3.8	[53]
	Esparto grass fiber	43.4	This study
TB	Turkish zeolite	64	[28]
	Gypsum	28	[54]
	Pulp fiber	25	[55]
	Flayash	6	[56]
	Esparto grass fiber	40	This study

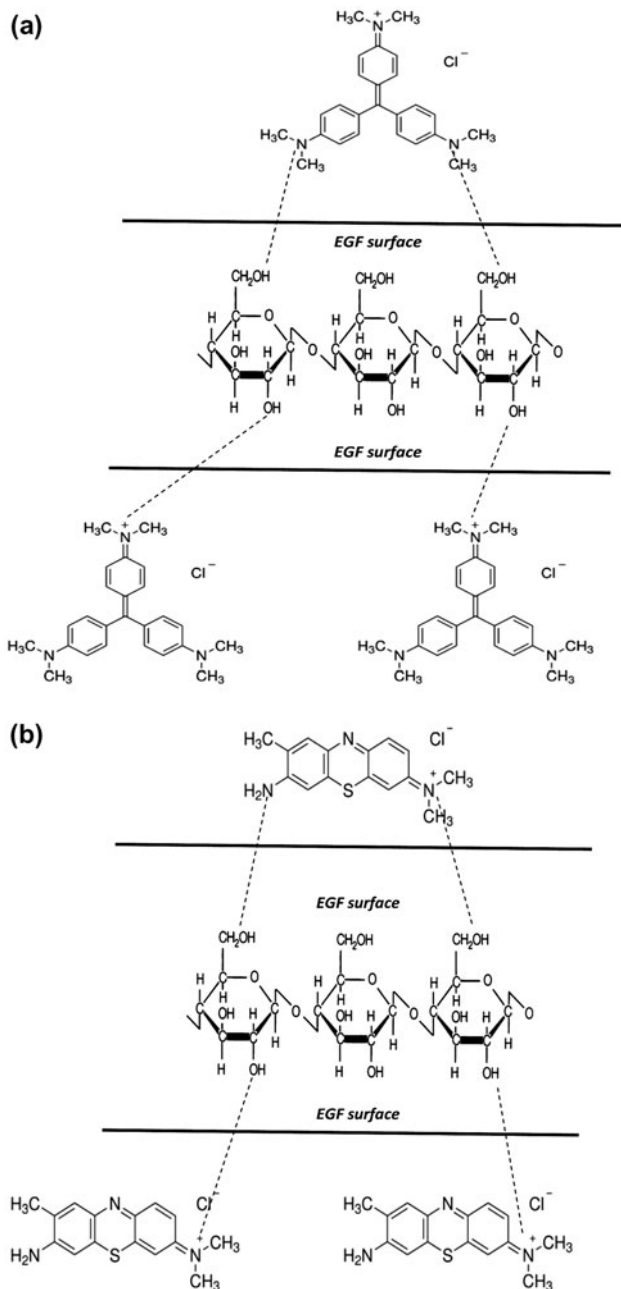


Fig. 12. Proposed mechanism for the biosorption of CV (a) and TB (b) onto EGF.

variation in adsorption capacities and affinities is mainly attributed to the differences in experimental condition and properties of adsorbent such as the specific surface area pore size and the nature of functional groups in adsorbents.

4. Conclusions

In this study, the potential of EGF as a natural biosorbent was investigated for removal of CV and TB from aqueous solution in the batch mode. The highest effectiveness of dyes removal was detected at pH 7.0. The equilibrium data of both dyes sorption were fitted by the Langmuir isotherm, and the kinetic ones referring to the period preceding the occurrence of equilibrium by the second-order-rate model. The related thermodynamic parameters demonstrated that the sorption of both dyes is an endothermic process.

Infrared spectroscopy demonstrated that several functional groups were involved in CV and TB binding on EGF. CV and TB sorption implied coordination to ester, hydroxyl, and amino groups and binding seemed to be related mainly to chemisorption with hydrogen atoms of non-ionized carboxyl groups.

The results of this investigation taken as a whole demonstrate the capacity of the EGF to remove CV and TB from aqueous solutions, which may then be proposed as a low-cost sorbent material used to reduce the impact of these dyes on the environment.

References

- [1] N. Mohan, N. Balasubramanian, C.A. Basha, Electrochemical oxidation of textile wastewater and its reuse, *J. Hazard. Mater.* 147 (2007) 644–651.
- [2] B.G.P. Kumar, L.R. Miranda, M. Velan, Adsorption of Bismark Brown dye on activated carbons prepared from rubberwood sawdust (*Hevea brasiliensis*) using different activation methods, *J. Hazard. Mater.* 126 (2005) 63–70.
- [3] A.K. Verma, R.R. Dash, P. Bhunia, A review on chemical coagulation/flocculation technologies for removal of colour from textile wastewaters, *J. Environ. Manage.* 93 (2011) 154–168.
- [4] P.K. Malik, S.K. Saha, Oxidation of direct dyes with hydrogen peroxide using ferrous ion as catalyst, *Sep. Purif. Technol.* 31 (2003) 241–250.
- [5] M. Koch, A. Yediler, D. Lienert, G. Insel, A. Kettrup, Ozonation of hydrolyzed azo dye reactive yellow 84 (CI), *Chemosphere* 46 (2002) 109–113.
- [6] G. Ciardelli, L. Corsi, M. Marucci, Membrane separation for wastewater reuse in the textile industry, *Resour. Conserv. Recycl.* 31 (2000) 189–197.
- [7] A.B. Dos Santos, F.J. Cervantes, J.B. Van Lier, Review paper on current technologies for decolourisation of textile wastewaters: Perspectives for anaerobic biotechnology, *Bioresour. Technol.* 98 (2007) 2369–2385.
- [8] F.C. Wu, R.L. Tseng, High adsorption capacity NaOH-activated carbon for dye removal from aqueous solution, *J. Hazard. Mater.* 152(3) (2008) 1256–1267.
- [9] N. Thinakaran, P. Baskaralingam, M. Pulikesi, P. Panneerselvam, S. Sivanesan, Removal of Acid Violet 17 from aqueous solutions by adsorption onto activated carbon prepared from sunflower seed hull, *J. Hazard. Mater.* 151 (2008) 316–322.
- [10] M.C. Ncibi, B. Mahjoub, M. Seffen, Kinetic and equilibrium studies of methylene blue biosorption by *Posidonia oceanica* (L.) fibres, *J. Hazard. Mater.* 139 (2007) 280–285.
- [11] G.O. El-Sayed, Removal of methylene blue and crystal violet from aqueous solutions by palm kernel fiber, *Desalination* 272 (2011) 225–232.
- [12] S. Irem, Q.M. Khan, E. Islam, A.J. Hashmat, M.A. ulHaq, M. Afzal, T. Mustafa, Enhanced removal of reactive navy blue dye using powdered orange waste, *Eco. Eng.* 58 (2013) 399–405.
- [13] G.Z. Kyzas, N.K. Lazaridis, A.C. Mitropoulos, Removal of dyes from aqueous solutions with untreated coffee residues as potential low-cost adsorbents: Equilibrium, reuse and thermodynamic approach, *Chem. Eng. J.* 189–190 (2012) 148–159.
- [14] M. Al-Ghouti, J. Li, Y. Salamh, N. Al-Laqtah, G. Walker, M.N.M. Ahmad, Adsorption mechanisms of removing heavy metals and dyes from aqueous solution using date pits solid adsorbent, *J. Hazard. Mater.* 176 (2010) 510–520.
- [15] S. Sadaf, H.N. Bhatti, Batch and fixed bed column studies for the removal of Indosol Yellow BG dye by peanut husk, *J. Taiwan. Inst. Chem. Eng.* 45 (2014) 541–553.
- [16] S. Sadaf, H.N. Bhatti, S. Ali, K-ur Rehman, Removal of Indosol Turquoise FBL dye from aqueous solution by bagasse, a low cost agricultural waste: Batch and column study, *Desalin. Water Treat.* 52 (2014) 184–198.
- [17] A. Mittal, V. Thakur, V. Gajbe, Adsorptive removal of toxic azo dye Amido Black 10B by hen feather, *Environ. Sci. Pollut. Res.* 20 (2013) 260–269.
- [18] V.K. Gupta, A. Mittal, D. Jhare, J. Mittal, Batch and bulk removal of hazardous colouring agent Rose Bengal by adsorption techniques using bottom ash as adsorbent, *RSC. Adv.* 2 (2012) 8381–8389.
- [19] A. Mittal, D. Jhare, J. Mittal, Adsorption of hazardous dye Eosin Yellow from aqueous solution onto waste material de-oiled soya: Isotherm, kinetics and bulk removal, *J. Mol. Liq.* 179 (2013) 133–140.
- [20] A. Cerdà, The effect of patchy distribution of *Stipa tenacissima* L. on run off and erosion, *J. Arid. Environ.* 36 (1997) 37–51.
- [21] A. Ghojtane, Etude de la dynamique des nappes alfatières de Kasserine et caractérisation écophysiological de l'alfa (*Stipa tenacissima* L.) [Study of Kasserine Alfa Slicks and Ecophysiological Characterization of Alfa (*Stippa Tenacissima* L.)], Thèse de doctorat en sciences agronomiques [PhD thesis in Agronomical Sciences]. Institut National Agronomique de Tunisie [Agronomical National Institute of Tunisia], 2010, (INAT), p.296.
- [22] H. Nadji, M.C. Brochier Salon, C. Bruzzese, A. Benaboura, M.N. Belgacem, Chemical composition and pulp properties of Alfa (*Stipa tenacissima*), *Cell. Chem. Technol.* 2006. 40(1–2), 45–52.

- [23] J. Díaz-Terán, D.M. Nevskaja, A.J. López-Peinado, A. Jerez, Porosity and adsorption properties of an activated charcoal, *Colloids Surf. A* 187–188 (2001) 167–175.
- [24] J.M. Valente Nabais, C. Laginhas, M.M.L.R. Carrott, P.J.M. Carrott, A.V. Nadal Gisbert, Surface and porous characterisation of activated carbons made from a novel biomass precursor, the esparto grass, *Appl. Surf. Sci.* 265 (2013) 919–924.
- [25] M.C. Paiva, I. Ammar, A.R. Campos, R.B. Cheikh, A.M. Cunha, Alfa fibres: Mechanical, morphological and interfacial characterization, *Comp. Sci. Technol.* 67 (2007) 1132–1138.
- [26] A.A. El-Hendawy, Variation in the FTIR spectra of a biomass under impregnation, carbonization and oxidation conditions, *J. Anal. Appl. Pyrolysis* 75 (2006) 159–166.
- [27] S. Li, Removal of crystal violet from aqueous solution by sorption into semi-interpenetrated networks hydrogels constituted of poly (acrylic acid-acrylamide-methacrylate) and amylose, *Bioresour. Technol.* 101 (2010) 2197–2202.
- [28] S.K. Alpat, Ö. Özbayrak, Ş. Alpat, H. Akçay, The adsorption kinetics and removal of cationic dye, Toluidine Blue O, from aqueous solution with Turkish zeolite, *J. Hazard. Mater.* 151 (2008) 213–220.
- [29] Z. Chi, R. Liu, Y. Sun, M. Wang, P. Zhang, C. Gao, Investigation on the toxic interaction of toluidine blue with calf thymus DNA, *J. Hazard. Mater.* 175 (2010) 274–278.
- [30] P.J.M. Carrott, J.M.V. Nabais, M.M.L. Ribeiro Carrott, J.A. Pajares, Preparation of activated carbon fibres from acrylic textile fibres, *Carbon* 39 (2001) 1543–1555.
- [31] J. Rouquerol, C.W. Fairbridge, D.H. Everett, J.H. Haynes, N. Pernicone, J.D.F. Ramsay, K.S.W. Sing, K.K. Unger, Recommendations for the characterization of porous solids, *Pure Appl. Chem.* 66 (1994) 1739–1758.
- [32] M.C. Ncibi, V. Jeanne-Rose, B. Mahjoub, C. Jean-Marius, J. Lambert, J.J. Ehrhardt, Y. Bercion, M. Seffen, S. Gaspard, Preparation and characterisation of raw chars and physically activated carbons derived from marine *Posidonia oceanica* (L.) fibres, *J. Hazard. Mater.* 165 (2009) 240–249.
- [33] F.F. Avelar, M.L. Bianchi, M. Gonçalves, E.G. da Mota, The use of piassava fibers (*Attalea funifera*) in the preparation of activated carbon, *Bioresour. Technol.* 101 (2010) 4639–4645.
- [34] M. Kılıç, E. Apaydın-Varol, A.E. Pütün, Preparation and surface characterization of activated carbons from *Euphorbia rigida* by chemical activation with $ZnCl_2$, K_2CO_3 , $NaOH$ and H_3PO_4 , *Appl. Surf. Sci.* 261 (2012) 247–254.
- [35] M. Schwanninger, J.C. Rodrigues, H. Pereira, B. Hinterstoisser, Effects of short-time vibratory ball milling on the shape of FT-IR spectra of wood and cellulose, *Vib. Spectrosc.* 36 (2004) 23–40.
- [36] M. Åkerholm, L. Salmén, Interactions between wood polymers studied by dynamic FT IR spectroscopy, *Polymer* 42 (2001) 963–969.
- [37] R. Kumar, R. Ahmad, Biosorption of hazardous crystal violet dye from aqueous solution onto treated ginger waste (TGW), *Desalination* 265 (2011) 112–118.
- [38] S. Noreen, H.N. Bhatti, S. Nausheen, S. Sadaf, M. Ashfaq, Batch and fixed bed adsorption study for the removal of Drimarine Black CL-B dye from aqueous solution using a lignocellulosic waste: A cost affective adsorbent, *Ind. Crop. Produc.* 50 (2013) 568–579.
- [39] B.H. Hameed, A.A. Ahmad, N. Aziz, Isotherms, kinetics and thermodynamics of acid dye adsorption on activated palm ash, *Chem. Eng. J.* 133 (2007) 195–203.
- [40] A.W.M. Ip, J.P. Barford, G. McKay, Reactive Black dye adsorption/desorption onto different adsorbents: Effect of salt, surface chemistry, pore size and surface area, *J. Colloid. Inter. Sci.* 337 (2009) 32–38.
- [41] R. Gong, Y. Ding, M. Li, C. Yang, H. Liu, Y. Sun, Utilization of powdered peanut hull as biosorbent for removal of anionic dyes from aqueous solution, *Dyes Pigm.* 64 (2005) 187–192.
- [42] I. Langmuir, The constitution and fundamental properties of solids and liquids, *J. Am. Chem. Soc.* 38(11) (1916) 2221–2295.
- [43] H.M.F. Freundlich, Over the adsorption in solution, *J. Phys. Chem.* 57 (1906) 385–470.
- [44] M.J. Temkin, V. Pyzhev, Recent modifications to Langmuir isotherms, *Acta Physiochim. USSR* 12 (1940) 217–222.
- [45] K.M. Parida, A.C. Pradhan, Removal of phenolic compounds from aqueous solutions by adsorption onto manganese nodule leached residue, *J. Hazard. Mater.* 717 (2010) 358–764.
- [46] S. Lagergren, About the theory of so-called adsorption of soluble substances, *K. Sven. Vetenskapsakad. Handl.* 24 (1898) 1–39.
- [47] Y.S. Ho, G. McKay, Sorption of dye from aqueous solution by peat, *Chem. Eng. J.* 70 (1998) 115–124.
- [48] W.J. Weber, J.C. Morris, Kinetics of adsorption on carbon from solution, *J. Sanitary Eng. Div. Am. Soc. Chem. Eng.* 89 (1963) 31–59.
- [49] W.H. Cheung, Y.S. Szeto, G. McKay, Intraparticle diffusion processes during acid dye adsorption onto chitosan, *Bioresour. Technol.* 98 (2007) 2897–2904.
- [50] E. Rogge, Extraction et étude des propriétés physiques et mécaniques des fibres d'alfa (Esparto grass) en vue d'applications, textiles (2010) 35–36.
- [51] C. Kannan, N. Buvanewari, T. Palvannan, Removal of plant poisoning dyes by adsorption on tomato plant root and green carbon from aqueous solution and its recovery, *Desalination* 249 (2009) 1132–1138.
- [52] A. Saeed, M. Sharif, M. Iqbal, Application potential of grapefruit peel as dye sorbent: Kinetics, equilibrium and mechanism of crystal violet adsorption, *J. Hazard. Mater.* 179 (2010) 564–572.
- [53] S.D. Khattri, M.K. Singh, Colour removal from synthetic dye wastewater using a bioadsorbent, *Water Air Soil Pollut.* 120 (2000) 283–294.
- [54] M.A.R. Shahnaz, M. Qadri, S.A. Karima, M. Al-Mansoori, Adsorption studies of Toluidine Blue from aqueous solutions onto gypsum, *Chem. Eng. J.* 150 (2009) 90–95.
- [55] T.G.M. Van de Ven, K. Saint-Cyr, M. Allix, Adsorption of toluidine blue on pulp fibers, *Colloids Surf. A* 294 (2007) 1–7.
- [56] R.Y. Talman, G. Atun, Effects of cationic and anionic surfactants on the adsorption of toluidine blue onto fly ash, *Colloids Surf. A* 281 (2006) 15–22.